CrossMark

ORIGINAL ARTICLE

Physiological and anatomical responses of *Phyllostachys vivax* and *Arundinaria fortunei* (Gramineae) under salt stress

Wei Ge[1] · Ying Zhang[1,2] · Zhongyuan Sun[1] · Juan Li[1] · Guohua Liu[3] ·
Yanjun Ma[1] · Jian Gao[1]

Abstract This research was conducted in order to study salt tolerance of *Phyllostachys vivax* McClure and *Arundinaria fortunei* (Van Houtte) Riviere et C. Riviere. The effects of salinity stress on growth parameters, anatomical changes, and ion accumulation from two 1-year-old bamboo species under different salt treatments were investigated. The growths of *P. vivax* and *A. fortunei* were not severely inhibited when salt content was lower than 0.42%. Their structural properties of vascular tissue were affected, and both species showed decreases in vessel diameters and a higher vessel density under salt stress, but they could still maintain relatively stable anatomical structure in saline soils. Besides, the results indicated that Na^+ accumulation progressively increased for organs as salinity levels increased. In particular, the accumulation of Na^+ in underground organs was obviously higher than those in culms and leaves. The levels of K^+, Ca^{2+}, and Mg^{2+} in salt-stressed cells gradually decreased in response to the increase of Na^+. Overall, we concluded that *P. vivax* and *A. fortunei* had the ability to withstand salt stress.

Keywords Anatomical structure · Growth index · Ion accumulation · Saline environment

Abbreviations
ROS	Reactive oxygen species
SOD	Superoxide dismutase
APX	Ascorbate peroxidase
POD	Guaiacol peroxidase
MDA	Malondialdehyde
F_0	Minimum fluorescence
F_m	Maximum fluorescence
F_v	Variable fluorescence
Pn	Net photosynthetic rate
SEM	Scanning electron microscopy

Wei Ge, Ying Zhang, Zhongyuan Sun, Juan Li have contributed equally to this work.

✉ Jian Gao
gaojianicbr@163.com

1 Key Laboratory of Bamboo and Rattan Science and Technology of the State Forestry Administration, International Centre for Bamboo and Rattan, No. 8 Futong Dongdajie, Wangjing, Chaoyang District, Beijing 100102, People's Republic of China

2 China National Engineering Research Center for Information Technology in Agriculture, Room 818, Building A, Beijing Nongke Mansion, No. 11, Shuguang Huayuan Middle Road, Haidian District, Beijing 100097, People's Republic of China

3 Bamboo Research Institute, Nanjing Forestry University, No. 159 Longpan Road, Nanjing 210037, People's Republic of China

Introduction

Plants are subjected to various abiotic stresses during their life cycle (Turan 2012). Salinity, a major environmental stress that adversely affects the overall metabolic activities of plants, can even cause death (Roychoudury et al. 2008). Salinity in soil or water is a major stress, especially in arid and semi-arid regions (Ashraf and Harris 2004; Mahajan and Tuteja 2005; Wang et al. 2013). Nearly 20% of global cultivated areas, and nearly half of global irrigated lands are affected by salinity (Zhu 2001). Soil contaminated by salts (ECe >4 dS m^{-1} or 40 mM NaCl or osmotic potential <0.117 MPa) are defined as salinized, which directly affects vegetative plant growth and development prior to

the reproductive stage (Allakhverdiev et al. 2000; Sairam and Tyagi 2004; Chinnusamy et al. 2005; Ashraf et al. 2008; Ashraf 2009; Suriyan and Chalermpol 2009), ultimately causing diminished economic yield and quality (Sairam and Tyagi 2004). Salinity stress is caused by excess salts such as Na^+, Cl^- and plant growth is first impaired by osmotic stress, which is directly caused by high concentrations of ions in the soil, making it more difficult for plants to extract water from a saline environment (Munns 1993; Flowers and Colmer 2008; Satpal et al. 2012). In a second phase of salt stress, accumulation of high concentrations of salts within the plant damage cell function and structure and, finally, suppresses plant growth (Flowers et al. 1977).

Plant response to salinity is a complex set of traits which involves morphological, physiological, and cellular processes (Zhu et al. 2012). Biomass weight, leaf index and survival ratio of plants in saline soil have been commonly used for screening salt-tolerant genotypes of plants (Allen et al. 1994; Cuartero et al. 2006; Li et al. 2009). Many studies have been performed examining the mechanism of plant salt tolerance, including osmotic adjustment, ROS scavenging, ion homeostasis, and photosynthesis (Bowler et al. 1991; Shi et al. 2002; Tattini et al. 2002; Stepien and Johnson 2009). Moreover, some salt-responsive genes have been identified (Rathinasabapathi et al. 1997; Apse et al. 1999; Halfter et al. 2000; Zhang et al. 2012a).

The effect of salinity on root (An et al. 2003), leaf (Hu and Schmidhalter 2001; Kilic and Kabar 2007), and stem anatomy (Cavuoglu et al. 2008; Dolatabadian et al. 2011) has already been reported. Junghans et al. (2006) showed that high salt concentrations reduced cambial activity in *Populus euphratica Olivier*. Xylem thickness had an increase, and xylem formation and arrangement changed when soybean plants were grown under salinity stress, especially at high levels of salinity (Dolatabadian et al. 2011). Moreover, salinity reduced total leaf area in strawberry plants (Awang et al. 1993) and increased leaf thickness in tomato plants (Raafat et al. 1991). Salinity also reduced development of vascular tissue (Belda and Ho 1993), increased trichome density, but decreased or had no effect on stomatal density in tomato.

Bamboo is one of the most important non-timber forest products with great ecological and economic values globally (Judziewicz et al. 1999). Bamboo belongs to the monophyletic BEP clade (Bambusoideae, Ehrhartoideae, Pooideae) in the grass family (Gramineae) and consists of woody and herbaceous varieties (Zhang et al. 2012b). These fast growing, resilient, perennial grasses have been shown to thrive in diverse climatic and soil conditions (Liese 1987). The bamboo resource in China is one of the richest in the world. More than 500 different bamboo

species occur (36% of the world total), and China is regarded as the center of bamboo origination and distribution worldwide (Dai et al. 2011; Zhou et al. 2011).

Phyllostachys vivax McClure belongs to Phyllostachys in the Bambusoideae. It is widely distributed in Jiangsu Province. *Phyllostachys vivax* likes the humid environment and could grow in coastal saline areas with strong adaptability. The wall of culm which is thin and brittle could be used to make baskets. It is one of the most important shoot bamboos because of its strong ability to produce new shoots and delicious taste (Li et al. 2012). *Arundinaria fortunei* (Van Houtte) Riviere et C. Riviere belongs to Pleioblastus in the Bambusoideae. It is widely distributed in East China. *Arundinaria fortune*i, a relatively cold-resistant plant, enjoys the humid environment and well drained soil (Zhang et al. 2006). It is an ornamental bamboo with short and glabrous internodes. Its culm sheaths are glabrous, and each culm has 4–7 lanceolate leaves that are white to pale yellow (Wu and Peter 2008). *Arundinaria fortunei* has good adaptability, fast growth, large root system, resistance to cutting, and few pests and diseases (Zhang et al. 2006).

In bamboo, salinity stress inhibits seedling growth, reduces shoots, and decreases biomass accumulation. Many studies on activities of SOD (superoxide dismutase), APX (ascorbate peroxidase), and POD (guaiacol peroxidase), accumulation of malondialdehyde (MDA), and photosynthesis and chlorophyll amounts have been reported. Unfortunately, there have been few studies on the effect of salinity on morphology and anatomy of bamboo. The studies on the effects of salinity on anatomy and ion concentration changes in different organs exhibit more sensitive responses compared with physiological and biochemical changes. Thus, we investigated (1) growth parameters; (2) anatomical changes of roots, rhizomes, culms, and leaves; and (3) accumulations of Na^+, K^+, Ca^{2+}, and Mg^{2+} in roots, rhizomes, culms, and leaves of two bamboo species under different amounts of salt stress. The objectives of this study were to evaluate their growing performances on salty soils by examining their salt tolerance from anatomical changes and ion accumulation.

Materials and methods

Determination of soil properties

Dongtai Forest Farm coastal beach shelter belts are located at N32°85′–34°20′; E119°57′–120°45′ in Yancheng City in Jiangsu Province. The soil in this zone is coastal saline soil, for which ingress of sea water is the major contributing factor in saline soil formation. We defined three regions as S1, S2, and S3 based on soil properties, including soil bulk

density, soil moisture content, pH and concentration of Na^+, K^+, Ca^{2+}, Mg^{2+}, Cl^-, NO_3^-, HCO_3^-, and SO_4^{2-}. The S1 area was on the coast. S2 and S3 were, respectively, 50 and 100 m from the coast.

Sample preparation

Roots, rhizomes, culms and leaves were collected from 1-year-old *P. vivax* and *A. fortunei*. Three sample plots of 10×10 m^2 were created in each area. Plant heights and ground diameters of all bamboo were measured in every sample plot. A 1-m^2 bamboo bundle containing standard bamboo was selected to determine biomass. Roots, rhizomes, culms, and leaves of bamboo were weighed. Three replicates were done in every sample plot.

A part of each sample was placed in an FAA buffer for microscopic analysis as described below. The remaining roots, rhizomes, culms, and leaves were washed three times with distilled water and quick-killed at 105 °C for 15 min; samples were then dried at 80 °C in an oven until dry weight remained constant. Metal elements were analyzed by inductively coupled plasma-mass spectrometry (ICP-MS). All samples were collected randomly and processed in sets of three replicates.

Measurements of photosynthetic parameters

Chlorophyll fluorescence quenching analysis was conducted with a portable fluorometer (Mini-IMAGING-PAM, WALZ, Germany). Leaves were darkened for half an hour before measurement. Minimum fluorescence (F_0) was found with the excitation of leaves with a weak light beam (0.5 μmol m^{-2} s^{-1}). Maximum fluorescence (F_m) was measured following a saturating pulse (2500 μmol m^{-2} s^{-1}). Yield of variable fluorescence (F_v) was calculated as F_m–F_0, and maximum efficiency of PSII photochemistry in the dark-adapted state as $F_v F_m = (F_m–F_0 F_m^{-1})$ (Genty et al. 1989). Net photosynthetic rate (Pn) was determined with LI-6400 (LI-COR, Lincoln, USA). All measurements were repeated at least three times.

Sectioning and SEM microscopy

Culm tissue samples of ~ 0.5 cm^3 in volume were fixed in FAA buffer [50% ethanol, acetic acid, and formaldehyde, 18:1:1 (v/v/v)] and exhausted with an aspirator pump. Subsequently, tissues were lyophilized by freeze-drying (Free Zone, LABCONCO, USA) for 48 h. Rhizome and culm sections were cut with a cryo-microtome (CM3050S, LEICA, Germany), while leaf and root sections were cut with a sliding microtome (SM2000R, LEICA, Germany). For scanning electron microscopy (SEM), root, culm, leaf and rhizome sections of each species were mounted onto

stubs with double-sided adhesive tape. Each sample was coated with gold in a Polaron E-5000 sputter coating unit, scanned, and photographed using an XL-30 ESEM (XL-30 ESEM, FEI, USA). The measurements were based on approximately 15 readings for each sample.

The anatomical indicators of roots, including exodermal thickness, endodermal thickness, and vessel diameter, were measured using Image-Pro Plus image-processing software (IPP). Vascular bundle area, sieve tube area, and vessel diameters for culms and rhizomes; and thickness of leaf, vascular bundle diameter, and vessel diameter in different leaf veins were also measured.

Inductively coupled plasma-mass spectrometry

The roots, rhizomes, culms, and leaves of *P. vivax* and *A. fortunei* were, respectively, collected in S1, S2 and S3; samples were washed first with tap water for 30 s and then twice with distilled water for 1 min to remove ions attached to surfaces. Cleaned samples were quick-killed at 105 °C for 15 min, and then dried in an oven at 80 °C until dry weight was constant, and K, Ca, Na, and Mg concentrations in samples were measured by ICP-MS. The samples were dried in an oven at 60 °C for 4 h before digestion. Prior to the determination of iron, 0.2 g of the sample was diluted with 5 ml of concentrated HNO_3 and mineralized by the microwave digestion system, using a multiwave 3000 with 1000 W of power at 15 ramp/min, followed by a 20-min hold at a rate of 0.4 bar s^{-1} up to 50 bars, in the temperature range of 213–230 °C. K, Ca, Na, and Mg concentrations were determined in these samples by the ICP-MS technique performed using an ICE3500 spectrometer (ICE3500, Thermo Scientific, USA). Each treatment was repeated three times, and data are reported as mean $\pm$ SD ($n = 3$).

Statistical analyses

Mean $\pm$ SD were determined. Analyses were conducted by SPSS software. Data from different replicates were analyzed by ANOVA and significant differences between means were determined by Duncan's multiple-range test, with differences of $P < 0.05$ being considered as significant.

Results

Analysis of soil physical properties

The soil bulk density of topsoil between 0 and 20 cm was 1.207–1.246 g cm^3, which is a typical sandy soil. The pH of soil was from 7.97 to 8.15, which is weakly alkaline.

Moreover, the ionic components of soil were mainly K^+, Ca^{2+}, Na^+, Mg^{2+}, Cl^-, SO_4^{2-}, CO_3^{2-}, and HCO_3^-, and concentrations of Na^+, Mg^{2+}, and Cl^- were highest (Table 1). Soluble salt contents of soil in the S1 area (soil near the ocean) ranged from 0.4 to 0.6%, being a saline soil. Soil in S2 was a mid-saline soil, and soluble salt contents ranged from 0.1 to 0.3%. The soluble salt concentrations of soils in S3 (soil far from the ocean) were less than 0.1%, being a non-saline soil.

Growth parameters of two species affected by salt stress

When uniformly one-year-old *P. vivax* and *A. fortunei* were cultured in soil with different salt concentrations, growth rates displayed measurable differences. In general, heights, diameter at breast height (DBH) and water content in different organs declined with increasing salt concentrations in soil. Growth characteristics of two species were not significantly affected by increasing salinity level to moderate levels (less than 0.1%) in soil far from the ocean (S3). However, at the high salt concentration level (from 0.3 to 0.6%), all of the recorded growth attributes were decreased, and there were lower values in *A. fortunei*. Growth of *A. fortunei* was more sensitive to NaCl stress, and height in soil of the nearshore area (S1) was significantly inhibited by 57%. Water contents in different organs of *A. fortunei* were obviously reduced in S2 and S1 soil; the reduction of leaf water contents was 36% in S2 and 44% in S1 (Table 2). Growth performance of *P. vivax* in the stressful environment was significantly affected; the decline in heights in S2 and S1 were 11 and 30%, respectively, and the reduction of leaf water contents in S2 and S1 were 13 and 27%, respectively. The effects of salt on biomass varied with concentration of salt (Table 3). The biomass of bamboo in S1 was inhibited significantly ($P < 0.05$) versus that in S3. The leaves of *P. vivax* were most affected by salt stress, the biomass of which decreased by 79%, with culms reduced by 59%. Performances of roots and rhizomes in the stressed environment were consistent with that of leaves, and the water content of rhizomes was more sensitive than roots. In conclusion, growth performance of *P. vivax* was highly affected by saline environments, while growth of *A. fortunei* was not affected greatly. Both *P. vivax* and *A. fortunei* could live in the saline environments, indicating that the two species both have high salt tolerance.

Effects of salt on photosynthetic parameters

The variation on photosynthetic parameters, as revealed by the $F_v F_m^{-1}$ ratio and Pn, indicates the toxicity of salt stress. There were no significant differences in P_n and

Table 1 Physical properties and salt contents of soils from three regions

Location	Treatment	Soil layer (cm)	Soil bulk density (g cm⁻³)	Soil moisture contents	PH	Total N (g kg⁻¹)	Total P (g kg⁻¹)	CO₃²⁻ (g kg⁻¹)	HCO₃⁻ (g kg⁻¹)	SO₄²⁻ (g kg⁻¹)	Cl⁻ (g kg⁻¹)	K⁺ (g kg⁻¹)	Ca²⁺ (g kg⁻¹)	Na⁺ (g kg⁻¹)	Mg²⁺ (g kg⁻¹)	Total soluble salt (g kg⁻¹)
Dongtai Forestry Farm	S1	0–20	1.241	0.357	8.11	0.912	0.753	0.100	0.091	0.261	1.753	0.088	0.202	1.571	0.187	4.285
		20–40	1.360	0.403	7.98	0.504	0.419	0.103	0.078	0.248	1.580	0.091	0.189	1.623	0.169	4.128
	S2	0–20	1.223	0.342	8.05	0.924	0.729	0.108	0.068	0.167	0.753	0.063	0.168	0.690	0.157	2.206
		20–40	1.382	0.413	8.02	0.485	0.428	0.095	0.083	0.179	0.841	0.054	0.156	0.531	0.163	2.136
	S3	0–20	1.260	0.354	8.13	0.895	0.737	0.093	0.076	0.140	0.152	0.043	0.132	0.168	0.113	0.975
		20–40	1.408	0.408	7.95	0.511	0.409	0.112	0.089	0.139	0.148	0.051	0.128	0.162	0.105	0.983

Table 2 Various morphological indicators and water contents of different organs of *Phyllostachys vivax* and *Arundinaria fortunei* in different salinity soils

Treatment		Height (m)	DBH (cm)	Water contents of organs (%)				
				Root	Rhizome	Stump	Branch	Leaf
P. vivax	S1	6.06 ± 0.21b	2.49 ± 0.13b	0.34 ± 0.02b	0.43 ± 0.01b	0.40 ± 0.02b	0.33 ± 0.01b	0.44 ± 0.01b
	S2	7.72 ± 0.62a	3.11 ± 0.20ab	0.42 ± 0.01a	0.49 ± 0.02b	0.49 ± 0.02a	0.41 ± 0.01a	0.53 ± 0.02a
	S3	8.66 ± 0.38a	3.61 ± 0.30a	0.45 ± 0.01a	0.55 ± 0.02a	0.52 ± 0.01a	0.45 ± 0.02a	0.61 ± 0.01a
A. fortunei	S1	0.32 ± 0.04c		0.33 ± 0.00b	0.38 ± 0.02c	0.35 ± 0.01c		0.29 ± 0.01c
	S2	0.41 ± 0.03b		0.34 ± 0.01b	0.40 ± 0.02b	0.38 ± 0.01b		0.33 ± 0.02b
	S3	0.75 ± 0.02a		0.46 ± 0.01a	0.63 ± 0.01a	0.53 ± 0.01a		0.52 ± 0.02a

Values followed by different letters differ significantly from each other ($P < 0.05$). Mean ± SE, $n = 3$

Distinct letters indicate significant ($P < 0.05$) differences

Table 3 Photosynthetic parameters and biomasses of different organs of *Phyllostachys vivax* and *Arundinaria fortunei* in different salinity soils

Treatment		Pn (μmol m^{-2} s^{-1})	F_v/F_m	Biomass of different organs (kg)			
				Root	Rhizome	Culm	Leaf
P. vivax	S1	1.15 ± 0.54b	0.75 ± 0.05b	8.10 ± 0.51b	5.72 ± 0.58b	3.76 ± 0.50c	0.42 ± 0.05b
	S2	2.59 ± 0.44a	0.78 ± 0.02ab	9.55 ± 0.56b	7.24 ± 0.53a	6.91 ± 0.50b	2.53 ± 0.50a
	S3	3.56 ± 0.25a	0.81 ± 0.02a	11.02 ± 1.00a	8.01 ± 0.86a	9.07 ± 0.48a	1.97 ± 0.50a
A. fortunei	S1	−0.34 ± 1.01b	0.69 ± 0.11b	1.57 ± 0.51a	3.37 ± 0.51b	0.49 ± 0.35a	0.53 ± 0.03a
	S2	0.26 ± 0.14a	0.74 ± 0.05ab	1.52 ± 0.52a	3.71 ± 1.23b	0.68 ± 0.25a	0.73 ± 0.02a
	S3	0.44 ± 0.31a	0.76 ± 0.07a	1.78 ± 1.23a	4.88 ± 0.52a	0.76 ± 0.50a	0.82 ± 0.02a

Values followed by different letters differ significantly from each other ($P < 0.05$). Mean ± SE, $n = 3$

Distinct letters indicate significant ($P < 0.05$) differences

$F_v F_m^{-1}$ of *P. vivax* and *A. fortunei* leaves in S2 compared to those in S3 (Table 3). With the increasing salt concentration, plants in S1 exhibited apparently lower values than those in S3. The obvious decrease showed that the leaf photosystem was damaged by high salt stress.

**Adjustment of anatomy changes to salt stress**

The scanning electron microscopic views of root cross sections of *P. vivax* (Figs. 1–6) and *A. fortunei* (Figs. 7–12) at different salinity levels are shown, including exodermis, parenchymal cells, aerenchyma, endodermis, vessels, and xylem tissue. The analysis of microscopic results showed a significant difference on all traits due to salinity stress between the two species. The increase in salinity levels increased the exodermis layer thickness of *P. vivax*. Exodermis thickness of *P. vivax* in S1 was 9.6% higher than that in S3 (Table 4). On the contrary, there was no significant difference among salinity treatments on exodermis thickness of *A. fortunei*. The exodermis is a layer of cells from the outermost layer of the cortex that provide protection against water loss of the root as well as

mechanical protection. Moreover, with the increasing salt content, the diameter of vessels were reduced, but significant differences existed between the two species. Reduction of vessel diameter in *P. vivax* was obvious in S1, where it declined by 13.8%. However, *A. fortunei* vessels were more sensitive to salinity stress, as the vessel diameter in S1 declined by 25.6% and by 12.8%, compared with S3. Moreover, salinity did not affect exodermis thickness in *A. fortunei*. Our results, which showed a significant increase thickness of exodermis with salt stress and weaker effect of salt stress on vessel diameter, led us to speculate that *P. vivax* would have a better tolerance to salt stress.

Bamboo plants have underground stems, which are commonly known rhizomes. The scanning electron microscopic views of rhizome cross sections from *P. vivax* (Figs. 13–18) and *A. fortunei* (Figs. 19–24) at different salinity levels are shown, including vessels, vascular bundles, parenchymal cells, and sieve tubes. Salinity-induced structural changes were seen in vascular tissue in rhizomes. With increasing salt, vascular bundle area and vessel diameter were decreased. Measured vascular tissue
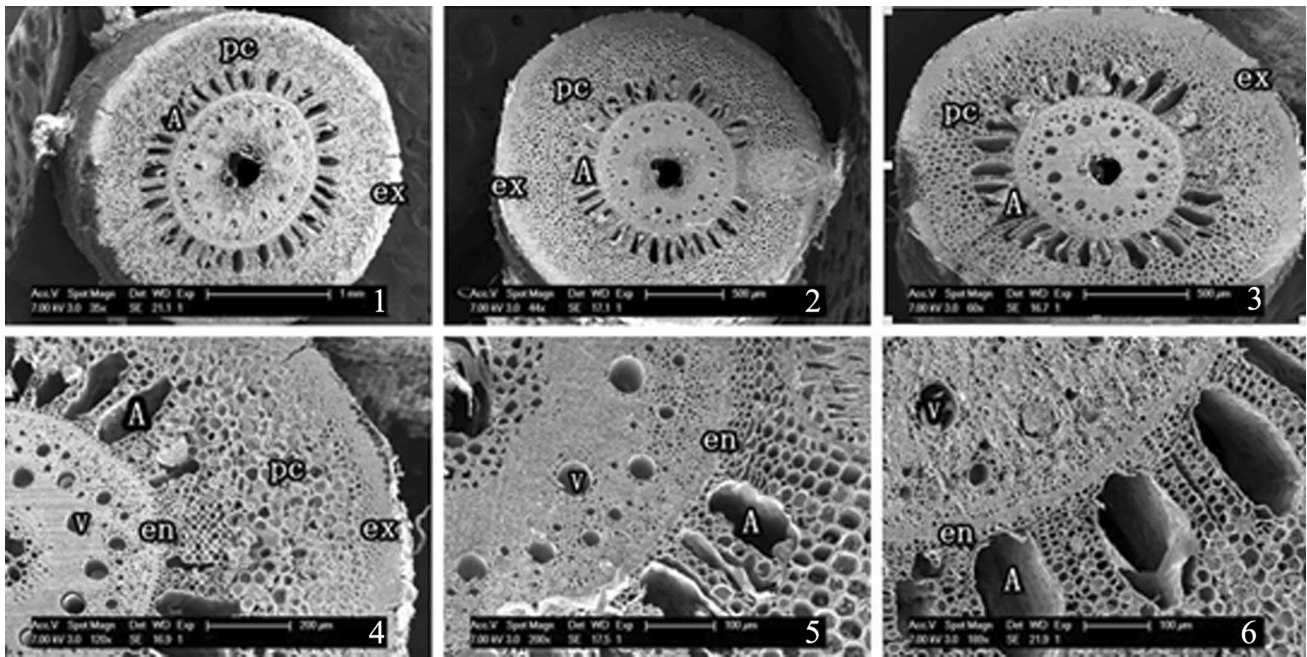
Figs. 1–6 The cross-sectional anatomy of roots of *Phyllostachys vivax* in different salinity soils **1**, **4**: S3; **2**, **5**: S2; **3**, **6**: S1. *en* endodermis, *ex* exodermis, *pc* parenchymal cell, *A* aerenchyma, *v* vessel
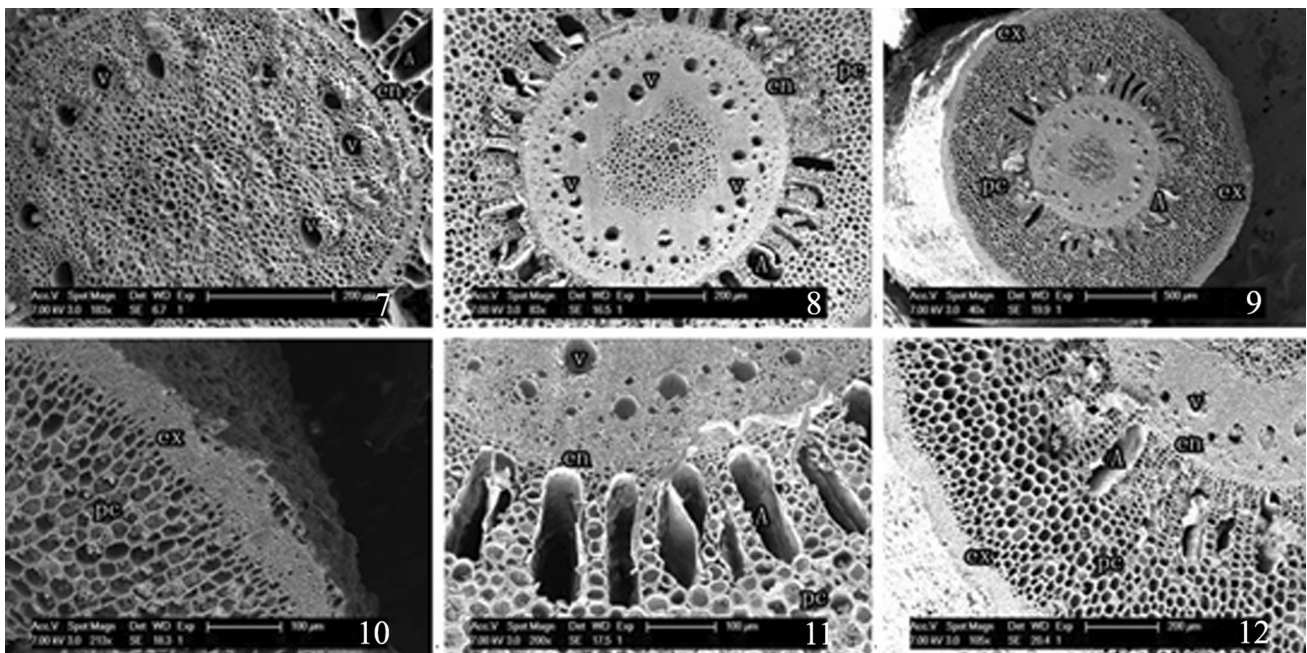
Figs. 7–12 The cross-sectional anatomy of roots of *Arundinaria fortunei* in different salinity soils **7**, **10**: S3; **8**, **11**: S2; **9**, **12**: S1. *en* endodermis, *ex* exodermis, *pc* parenchymal cell, *A* aerenchyma, *v* vessel

parameters in rhizomes of *P. vivax* were less affected by salt stress. The vascular bundle area of *P. vivax* and *A. fortunei* in S1 were diminished by 18.5 and 48.3%, respectively (Table 5). Changes in sieve tube area under salt stress was similar to those of the vascular bundle area (20.7 and 34.3%). The increase in salinity level decreased

the vessel diameter. The vessel diameter of *A. fortunei* had the highest decrease in S1, which was 26.2% lower than that in S3, while vessel diameter of *P. vivax* in S1 was declined by 11.2% compared with that in S3. Vascular area represents the ability of bamboo to transport water and organic nutrients. We believe that the decrease in vascular

Table 4 Anatomical cross-sectional characteristics of roots of *Phyllostachys vivax* and *Arundinaria fortunei* in different salinity soils

Treatment		Thickness of exodermis (µm)	Thickness of endodermis (µm)	Diameter of vessel (µm)
P. vivax	S1	110.48 ± 2.71a	29.12 ± 0.43a	69.96 ± 1.44b
	S2	105.98 ± 2.31b	22.29 ± 0.52b	78.10 ± 0.88a
	S3	100.79 ± 2.48c	22.54 ± 0.61b	81.21 ± 1.14a
A. fortunei	S1	89.40 ± 1.24a	21.96 ± 0.72a	44.18 ± 1.01c
	S2	89.47 ± 1.13a	20.43 ± 0.61a	51.77 ± 1.06b
	S3	86.65 ± 1.73a	18.07 ± 0.74b	59.38 ± 1.24a

Values followed by different letters differ significantly from each other ($P < 0.05$). Mean ± SE, $n = 3$

Distinct letters indicate significant ($P < 0.05$) differences
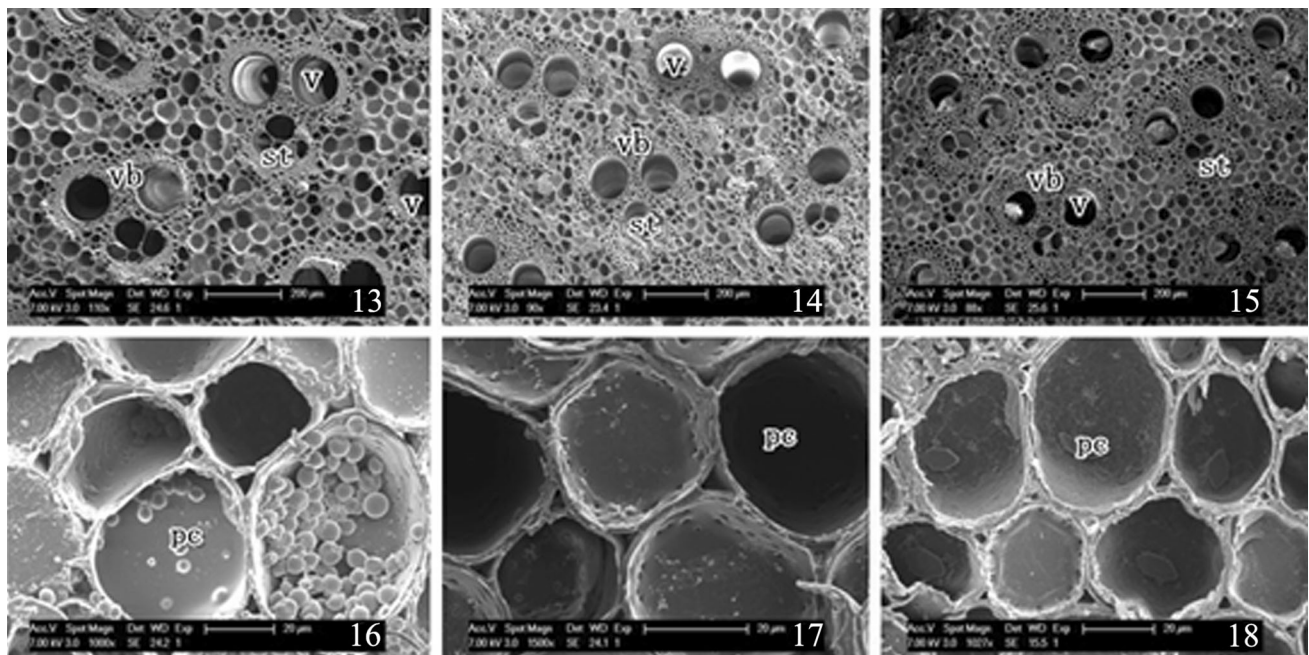
Figs. 13–18 The cross-sectional anatomy of rhizomes of *Phyllostachys vivax* in different salinity soils **13**, **16**: S3; **14**, **17**: S2; **15**, **18**: S1. *v* vessel, *vb* vascular bundle, *pc* parenchymal cell, *st* sieve tube

area directly reduced efficiency of transportation, and the plant growth was inhibited.

Vascular tissue in culms of *P. vivax* was structurally affected by salt stress (Figs. 25–30). Changes in vascular bundle area and sieve tube area of culms of *P. vivax* in S2 and S3 were not significantly different. Moreover, when the salt concentration increased to 0.3%, vascular bundle area and sieve tube area of culms in S1 declined by 11.96 and 9.38%, respectively, compared to those in S3 (Table 6). These parameters were not analyzed in *A. fortunei*.

There were also significant differences among salinity treatments in leaf parameters. With the increasing salt content, the leaf thickness reduced. Leaf thickness of *P. vivax* in S1 was reduced by 5.1%, which was not significantly different compared with S3. While leaves of *A. fortunei* were more sensitive to salinity stress, with leaf thickness of that in S1 declined by 28.3%. Leaf number or leaf area expansion appeared to be a sensitive indicator to salinity. Our research showed that salt-stressed plants have smaller vascular bundle diameters. Overall, vascular bundles of *P. vivax* were less affected (Table 7). Furthermore, trichome density from epidermal leaf cells of *P. vivax* (Figs. 31–36) and *A. fortunei* (Figs. 37–42) was observed to increase under the salt stress treatment.

Accumulation of Na$^+$, K$^+$, Ca^{2+} and Mg^{2+} in organs

The accumulation of Na$^+$, K$^+$, Ca^{2+} and Mg^{2+} in the organs of *P. vivax* and *A. fortunei* at various concentrations of salt were studied. Our results showed that Na$^+$ accumulation
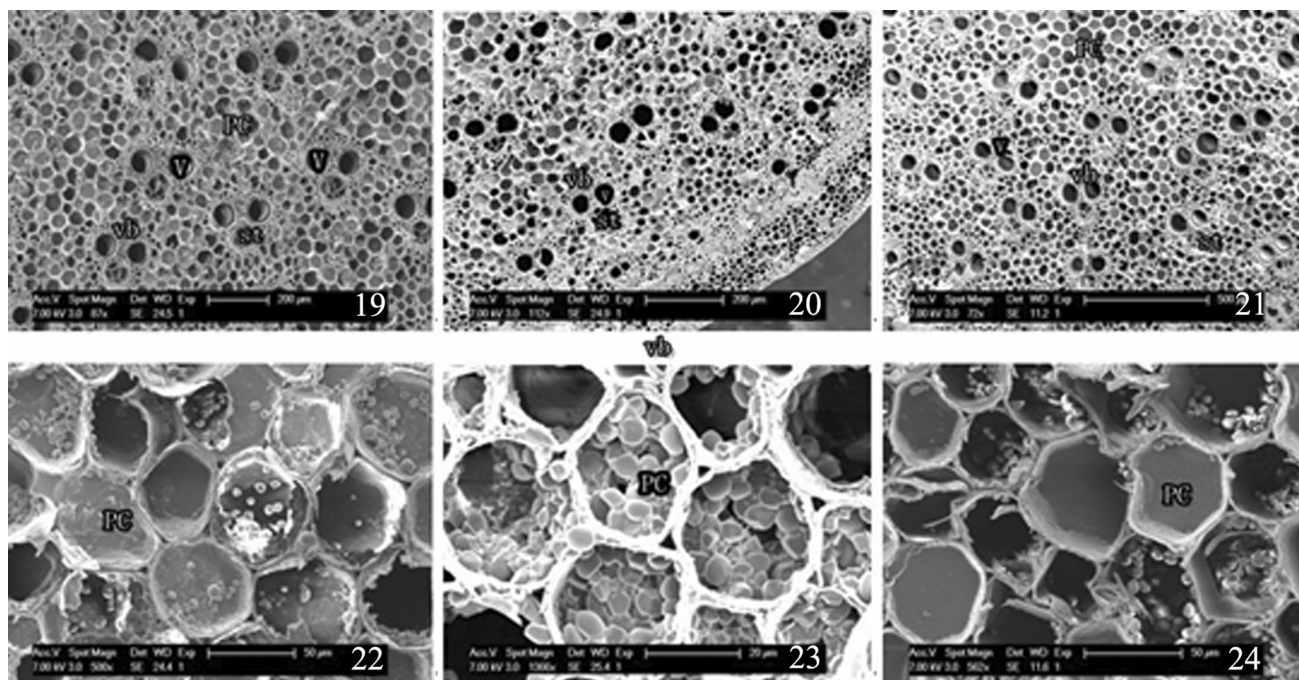
Figs. 19–24 The cross-sectional anatomy of rhizomes of *Arundinaria fortunei* in different salinity soils **19**, **22**: S3; **20**, **23**: S2; **21**, **24**: S1. *v* vessel, *vb* vascular bundle, *pc* parenchymal cell, *st* sieve tube

Table 5 Anatomical cross-sectional characteristics of rhizomes of *Phyllostachys vivax* and *Arundinaria fortunei* in different salinity soils

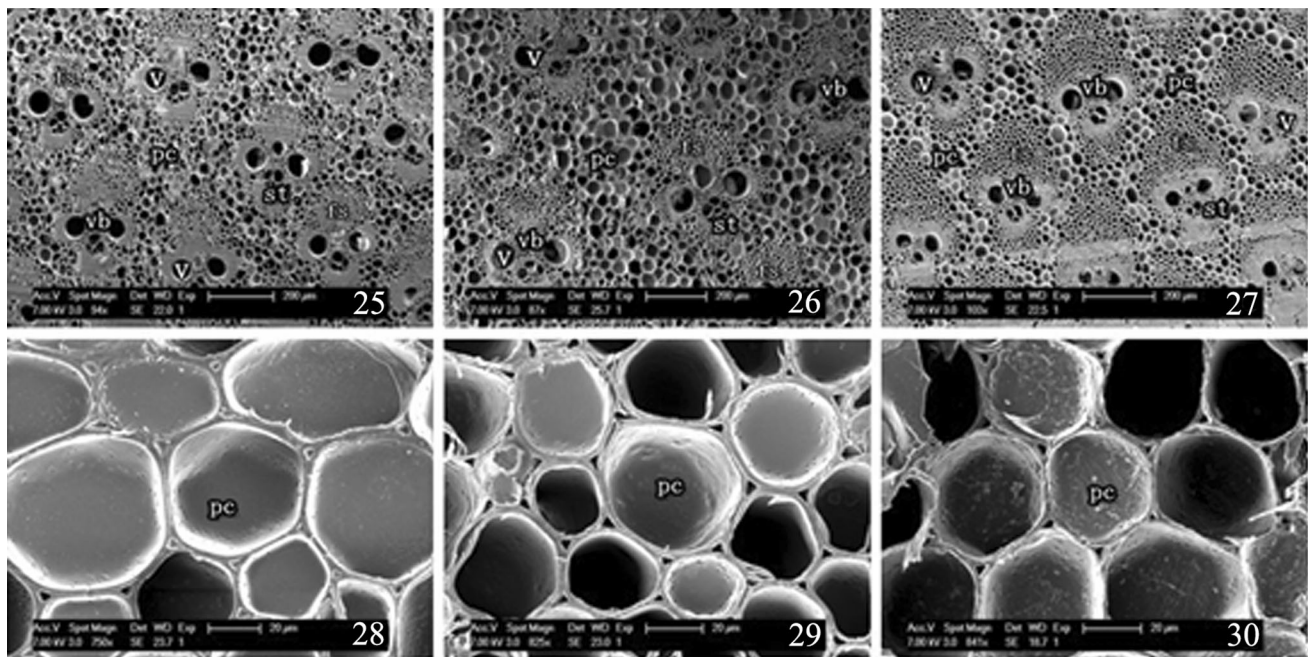| Treatment		Crosssectional area of vascular bundle (μm^2)	Crosssectional area of sieve tube (μm^2)	Diameter of vessel (μm)
P. vivax	S1	8.72E4 ± 1757.30b	7.01E3 ± 504.96b	98.90 ± 2.24c
	S2	1.16E5 ± 3072.03a	9.24E3 ± 407.95a	104.59 ± 2.60b
	S3	1.07E5 ± 3989.08a	8.84E3 ± 365.58a	111.33 ± 2.12a
A. fortunei	S1	1.87E4 ± 898.14c	2.45E3 ± 74.85b	48.02 ± 1.20c
	S2	2.78E4 ± 761.70b	2.77E3 ± 48.85b	55.23 ± 2.06b
	S3	3.62E4 ± 644.68a	3.73E3 ± 52.34a	64.99 ± 1.29a

Values followed by different letters differ significantly from each other ($P < 0.05$). Mean ± SE, $n = 3$

Distinct letters indicate significant ($P < 0.05$) differences

progressively increased for organs as salinity levels increased (Table 8). In particular, the accumulation of Na^+ in underground organs was significantly higher than that in culms and leaves. K^+ content decreased with the over-accumulation of Na^+. The K^+ efflux from organs of *P. vivax* tended to be smaller than that of *A. fortunei*. For example, K^+ concentration in leaves of *P. vivax* in S1 declined by 45.9%, while K^+ concentrations in leaves of *A. fortunei* in S1 zone decreased by 72.0%. The loss of K^+ content in leaves of *P. vivax* was much slower than *A. fortunei*. Salt stress also caused a decrease in Ca^{2+} concentration. The reductions of Mg^{2+} in leaves and roots were much larger than those in culms and rhizomes. For leaf Mg^{2+} content, our data revealed that the treated *A. fortunei* was reduced more. The Mg^{2+} content of roots showed the same pattern as that of leaves.

Discussion

Plant growth and development are adversely affected by salinity—a major environmental stress that limits agricultural production. The initial phase of growth reduction is due to an osmotic effect, which is similar to the initial response to water stress. The second, slower effect is the result of salt toxicity, and a salt-sensitive species or genotype differs from a more salt-tolerant one by its inability to prevent salt accumulation to toxic levels (Lauchli and Grattan 2007). High salinity in soil reduces the water potential of the rhizosphere environment, causing water stress in plants, which will result in difficulties in absorbing water and inhibition of plant growth. Therefore, the index of water content is an important indicator of the

Figs. 25–30 The cross-sectional anatomy of culms of *Phyllostachys vivax* in different salinity soils **25**, **28**: S3; **26**, **29**: S2; **27**, **30**: S1. *v* vessel, *vb* vascular bundle, *pc* parenchymal cell, *st* sieve tube

Table 6 Anatomical cross-sectional characteristics of culms of *Phyllostachys vivax* in different salinity soils

Treatment		Crosssectional area of vascular bundle (μm^2)	Crosssectional area of sieve tube (μm^2)	Diameter of vessel (μm)
P. vivax	S1	5.89E4 ± 2271.28b	4.35E3 ± 200.64b	80.79 ± 1.02b
	S2	6.33E4 ± 2140.91ab	4.61E3 ± 323.60ab	83.36 ± 0.60b
	S3	6.69E4 ± 2423.95a	4.80E3 ± 344.31a	89.40 ± 0.55a

Values followed by different letters differ significantly from each other ($P < 0.05$). Mean ± SE, $n = 3$

Distinct letters indicate significant ($P < 0.05$) differences

Table 7 Anatomical cross-sectional characteristics of leaves of *Phyllostachys vivax* and *Arundinaria fortunei* in different salinity soils

Treatment		Depth of leaf (μm)	Diameter of great vascular bundle (μm)	Diameter of small vascular bundle (μm)	Diameter of vessel (μm)
P. vivax	S1	75.19 ± 0.87a	54.77 ± 1.10b	29.16 ± 0.66b	12.83 ± 0.33b
	S2	77.18 ± 0.92a	60.65 ± 0.34a	31.49 ± 0.79ab	15.01 ± 0.25a
	S3	79.26 ± 1.50a	63.13 ± 0.85a	33.80 ± 0.40 a	15.29 ± 0.10a
A. fortunei	S1	85.12 ± 2.53c	69.66 ± 1.65b	35.10 ± 1.73c	13.87 ± 0.87b
	S2	93.99 ± 2.51b	75.19 ± 2.32b	39.11 ± 1.35b	14.36 ± 0.86b
	S3	118.65 ± 3.23a	91.99 ± 2.51a	43.94 ± 2.23a	18.19 ± 0.79a

Values followed by different letters differ significantly from each other ($P < 0.05$). Mean ± SE, $n = 3$

Distinct letters indicate significant ($P < 0.05$) differences

salt-tolerance mechanism, which is a direct reflection of osmotic stress affected by salinity and energy. In addition, adaptive responses in biomass production are significant tolerance indicators for bamboo for coping with a stressful environment. The accumulation of biomass was negatively correlated with salt concentration in the current research, indicating that both *P. vivax* and *A. fortunei* could tolerate low salt stress and were severely damaged by high salt stress. *P. vivax* and *A. fortunei* have the ability and potential to adapt to saline environments. In terms of root
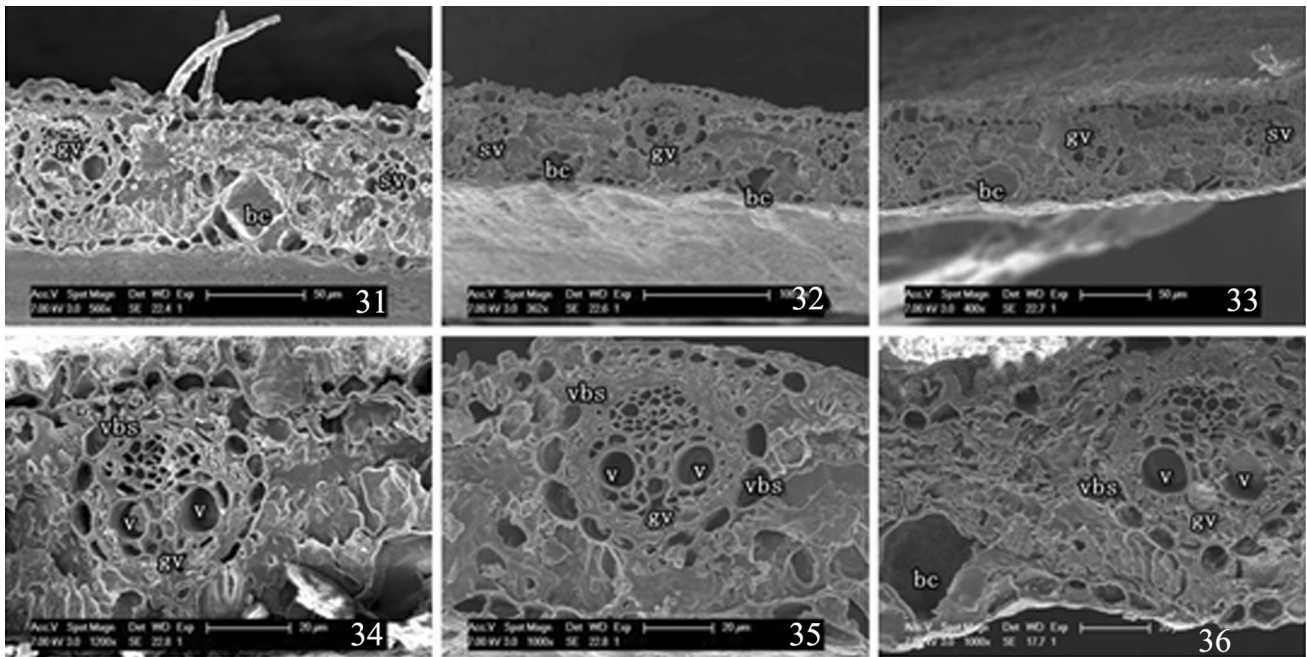
Figs. 31–36 The cross-sectional anatomy of leaves of *Phyllostachys vivax* in different salinity soils **31**, **34**: S3; **32**, **35**: S2; **33**, **36**: S1. *gv* great vascular bundle, *sv* small vascular bundle, *v* vessel, *bc* bulliform cell, *vbs* vascular bundle sheath
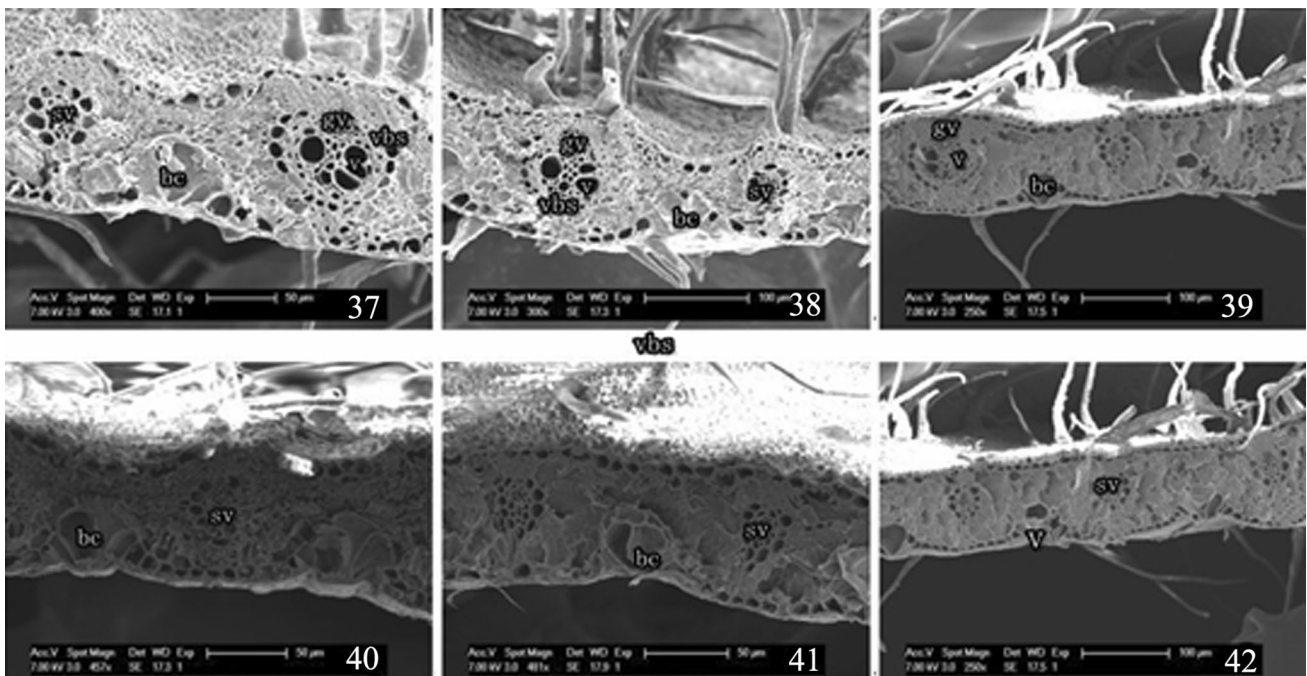
Figs. 37–42 The cross-sectional anatomy of leaves of *Arundinaria fortunei* in different salinity soils **37**, **40**: S3; **38**, **41**: S2; **39**, **42**: S1. *gv* great vascular bundle, *sv* small vascular bundle, *v* vessel, *bc* bulliform cell, *vbs* vascular bundle sheath

structure, the uptakes of water, minerals, and heavy metals are directly affected by root morphological characteristics (Marschner 1995). It indicates that the genotypic difference for salt tolerance had a close relationship with root morphology, fine root development, and physiological characters (Jia et al. 2008). In our results, increasing thickness

of the exodermis after salt stress may provide protection against water loss of the root, thus showing a higher tolerance to salinity stress. The xylem anatomy of plants is optimized to ensure a continuous transport of water from roots to leaves under varying water supply conditions. Drought and increased salinity impair the water status of a

Table 8 Ion concentration changes in four different organs of *Phyllostachys vivax* and *Arundinaria fortunei* under different amounts of soil salt

Treatment		Na$^+$ (mg g^{-1})	K$^+$ (mg g^{-1})	Ca^{2+} (mg g^{-1})	Mg^{2+} (mg g^{-1})
Roots of *P. vivax*	S1	1.10 ± 0.03a	4.70 ± 0.38b	0.45 ± 0.02b	0.79 ± 0.09b
	S2	0.76 ± 0.03b	6.93 ± 0.36a	0.72 ± 0.03ab	1.05 ± 0.02a
	S3	0.51 ± 0.06c	8.08 ± 0.62a	0.89 ± 0.09a	1.16 ± 0.07a
Roots of *A. fortunei*	S1	1.26 ± 0.03a	4.38 ± 0.29c	0.23 ± 0.01b	0.48 ± 0.02c
	S2	0.94 ± 0.03b	8.76 ± 0.14b	0.30 ± 0.01b	0.74 ± 0.01b
	S3	0.52 ± 0.03c	14.13 ± 0.84a	0.50 ± 0.09a	1.27 ± 0.06a
Rhizomes of *P. vivax*	S1	0.73 ± 0.01a	2.88 ± 0.07c	0.38 ± 0.02b	0.62 ± 0.01c
	S2	0.54 ± 0.02b	4.39 ± 0.11b	0.49 ± 0.05a	0.76 ± 0.02b
	S3	0.42 ± 0.00b	5.31 ± 0.20a	0.53 ± 0.03a	0.88 ± 0.02a
Rhizomes of *A. fortunei*	S1	0.94 ± 0.03a	3.51 ± 0.66b	0.24 ± 0.02b	0.42 ± 0.02b
	S2	0.71 ± 0.01b	5.11 ± 0.38b	0.20 ± 0.01b	0.68 ± 0.02b
	S3	0.40 ± 0.01c	10.33 ± 0.35a	0.43 ± 0.02a	1.15 ± 0.08a
Culms of *P. vivax*	S1	0.37 ± 0.02a	4.50 ± 0.31c	0.42 ± 0.02b	0.62 ± 0.03b
	S2	0.27 ± 0.02b	7.55 ± 0.75b	0.51 ± 0.03b	0.79 ± 0.02a
	S3	0.21 ± 0.01b	9.41 ± 0.34a	0.72 ± 0.05a	0.85 ± 0.03a
Culms of *A. fortunei*	S1	0.74 ± 0.01a	2.92 ± 0.13c	0.20 ± 0.01c	0.44 ± 0.01c
	S2	0.58 ± 0.04b	5.20 ± 0.11b	0.32 ± 0.02b	0.77 ± 0.05b
	S3	0.32 ± 0.02c	9.12 ± 0.25a	0.45 ± 0.07a	1.33 ± 0.06a
Leaves of *P. vivax*	S1	0.41 ± 0.04a	5.67 ± 0.51b	0.34 ± 0.03c	1.41 ± 0.05c
	S2	0.30 ± 0.01b	9.21 ± 0.35a	0.45 ± 0.00b	1.79 ± 0.09b
	S3	0.25 ± 0.03b	10.48 ± 0.22a	0.58 ± 0.01a	2.11 ± 0.09a
Leaves of *A. fortunei*	S1	0.67 ± 0.01a	2.33 ± 0.20b	0.27 ± 0.02b	0.50 ± 0.00c
	S2	0.55 ± 0.01b	3.57 ± 0.62b	0.36 ± 0.03b	0.86 ± 0.02b
	S3	0.24 ± 0.01c	8.32 ± 0.56a	0.67 ± 0.05a	1.60 ± 0.04a

Values followed by different letters differ significantly from each other ($P < 0.05$). Mean ± SE, $n = 3$

plant and may increase the tension on the water column in the conducting system, which makes the occurrence of cavitations and subsequent embolisms more likely (Tyree and Sperry 1989; Zimmermann and Tyree 2002). The xylem of plants exposed to high salinity often contain vessels with smaller diameters than those plants grown under less stressful conditions (Fahn 1964; Bass et al. 1983; Reinhardt and Rost 1995; Baum et al. 2000). A similar phenomenon was observed by Eckstein et al. (1976), who investigated the effect of deicing salt on chestnut trees. They found smaller and more rounded vessels and a higher vessel density under high salinity. In the present study, both species showed decreases in vessel diameters and a higher vessel density under salt stress. Moreover, trichomes may be a mechanism to increase tolerance to salt stress. It was recently suggested that leaf glandular trichomes could contribute to high salt tolerance by the excretion of ions (Gucci et al. 1997).

Photosynthetic parameters mainly depend on the photosynthetic ability and pigment content of leaves (Gitelson et al. 1999). Thus, they have been widely used in the analysis of photosynthesis ability, the study of the photosynthetic mechanism and the identification of leaf injuries. Important photosynthetic parameters, such as the $F_v F_m^{-1}$ ratio and Pn, often decrease when plants are damaged or experiencing stress because of photo-inhibition from a stressful environment. In the investigation, $F_v F_m^{-1}$ and Pn declined in leaves of *P. vivax* and *A. fortunei* exposed to high salt concentrations. The decrease indicates that the salt-stress environment could inhibit photosynthesis by damaging the reaction center of photosynthesis (Maxwell and Johnson 2000). Indeed, photosynthesis of *P. vivax* and *A. fortunei* leaves were both severely constrained in S1.

According to Weimberg (1987), high levels of Na$^+$ inside cells inhibit K$^+$ uptake, and as a result, it causes an increase in the Na$^+$/K$^+$ ratio. Under saline conditions, the ratio falls dramatically due to excessive Na$^+$ accumulation in the cytosol and K$^+$ leakage (Maathuis and Amtmann 1999; Cuin et al. 2008). The ability to retain K$^+$ makes an important contribution to plant salt tolerance (Chen et al. 2007; Summart et al. 2010). Decrease of cytosolic K$^+$ may activate caspase-like proteases leading to programmed cell

death (Shabala 2009). Therefore, the ability to retain high concentrations of K^+ in leaves presumably in the cytosol is likely to be important for maintaining normal metabolism of leaves under salt stress (Zhang et al. 2011).

K^+ and Ca^{2+} have been reported to be major cations in cell organization as well as major contributors to osmotic adjustment under stress conditions in several plant species (Santos-Diaz and Alejo-Ochoa 1994; Hirschi 2004). In the current study, the level of K^+ and Ca^{2+} in salt-stressed cells gradually decreased while that of Na^+ dramatically increased. The decrease in K^+ and Ca^{2+} contents under stress condition has been previously reported in other species particularly in the salt-sensitive lines (Lutts et al. 1996; Lutts et al. 2004).

Mg^{2+}, an important element for chlorophyll structure and as an enzyme cofactor, is found in photosynthate export, which is impaired and leads to enhanced degradation of chlorophyll in magnesium-deficient source leaves, resulting in increased oxygenase activity of ribulose bisphosphate carboxylase (Marschner and Cakmak 1989; Ramoliya et al. 2004). Mg^{2+} accumulations in leaves and roots were significantly decreased. The decrease may be attributed to the fact that increasing Na^+ ions inhibited the absorption of both K^+ and Mg^{2+} due to antagonistic interactions (Correia et al. 2010).

In conclusion, by investigating the growth indexes, anatomical indicators, and elemental distributions of the two species in three different saline areas, our study showed that they exhibited good growth performance and stable anatomical structure in saline soils. In addition, they had less accumulation of Na^+ and degree of nutrient elements imbalance. Thus, we conclude that *P. vivax* and *A. fortunei* have the ability to grow successfully in salty soils.

References

Allakhverdiev SI, Sakamoto A, Nishiyama Y, Inaba M, Murata N (2000) Ionic and osmotic effects of NaCl-induced inactivation of photosystems I and II in *Synechococcus* sp. Plant Physiol 123:1047–1056

Allen JA, Chambers JL, Stine M (1994) Prospects for increasing the salt tolerance of forest tress: a review. Tree Physiol 14:843–853

An P, Inanaga S, Li X, Schimizu H, Tanimoto E (2003) Root characteristics in salt tolerance. Root Res 12:125–132

Apse MP, Aharon GS, Snedden WA, Blumwald E (1999) Salt tolerance conferred by overexpression of a vacular Na^+/H^+ antiport in *Arabidopsis*. Science 285:1256–1258

Ashraf M (2009) Biotechnological approach of improving plant salt tolerance using antioxidants as markers. Biotech Adv 27:84–93

Ashraf M, Harris PJC (2004) Potential biochemical indicators of salinity tolerance in plants. Plant Sci 166(1):3–16

Ashraf M, Athar HR, Harris PJC, Kwon TR (2008) Some prospective strategies for improving crop salt tolerance. Adv Agron 97:45–110

Awang YB, Atherton JG, Taylor AJ (1993) Salinity effects on strawberry plants in rockwool. 1. Growth and leaf water relations. J Hortic Sci 68:783–790

Bass P, Werker E, Fahn A (1983) Some ecological trends in vessel characters. IAWA Bull 4:141–159

Baum SF, Tran PN, Silk WK (2000) Effects of salinity on xylem structure and water use in growing leaves of sorghum. New Phytol 146:119–127

Belda RM, Ho LC (1993) Salinity effects on the network of vascular bundles during tomato fruit development. J Hortic Sci 68:557–564

Bowler C, Slooten L, Vandenbranden S, De Rycke R, Botterman J, Sybesma C, Van Montagu M, Inze D (1991) Manganese superoxide dismutase can reduce cellular damage mediated by oxygen radicals in transgenic plants. EMBO J 10:1723–1732

Cavuoglu K, Kilic S, Kabar K (2008) Effects of some plant growth regulators on leaf anatomy of radish seedlings grown under saline conditions. JABS 2:47–50

Chen ZH, Zhou MX, Newman IA, Mendham NJ, Zhang GP, Shabala S (2007) Potassium and sodium relations in salinized barley tissues as a basis of differential salt tolerance. Funct Plant Biol 34:150–162

Chinnusamy V, Jagendorf A, Zhu JK (2005) Understanding and improving salt tolerance in plants. Crop Sci 45:437–448

Correia PJ, Gama F, Pestana M, Martins-Louc MA (2010) Tolerance of young (*Ceratonia siliqua* L.) carob rootstock to NaCl. Agr Water Manage 97:777–938

Cuartero J, Bolarin MC, Asins MJ, Mormeno V (2006) Increasing salt tolerance in the tomato. J Exp Bot 57:1045–1058

Cuin TA, Betts SA, Chalmandrier R, Shabala S (2008) A root's ability to retain K^+ correlates with salt tolerance in wheat. J Exp Bot 59:2697–2706

Dai L, Wang Y, Su D, Zhou L, Yu D, Lewis B, Qi L (2011) Major forest types and the evolution of sustainable forestry in china. Environ Manag 48:1066–1078

Dolatabadian A, Modarressanavy SAM, Ghanati F (2011) Effect of salinity on growth, xylem structure and anatomical characteristics of soybean. Notulae Sci Biol 3:41–45

Eckstein D, Liese W, Parameswaran N (1976) On the structural changes in wood and bark of a salt-damaged horsechestnut tree. Holzforschung 30:173–178

Fahn A (1964) Some anatomical adaptations of desert plants. Phytomorphology 14:93–102

Flowers TJ, Colmer TD (2008) Salinity tolerance in halophytes. New Phytol 179:945–963

Flowers TJ, Troke PF, Yeo AR (1977) The mechanism of salt tolerance in halophytes. Annu Rev Plant Physiol 28:89–121

Genty B, Briantais JM, Baker NR (1989) The relationship between the quantum yield of photosynthetic electron transport and quenching of chlorophyll fluorescence. Biochem Biophys Acta 99:87–92

Gitelson AA, Buschmann C, Lichtenthaler HK (1999) The chlorophyll fluorescence ratio F735/F700 as an accurate measure of the chlorophyll content in plants. Remote Sens Environ 69:296–302

Gucci R, Aronne G, Lombardini L, Tattini M (1997) Salinity tolerance in *Phillyrea* species. New Phytol 135:227–234

Halfter U, Ishitani M, Zhu JK (2000) The Arabidopsis SOS2 protein kinase physically interacts with and is activated by the calcium-binding protein SOS3. Proc Natl Acad Sci USA 97:3735–3740

Hirschi KD (2004) The calcium conundrum, both versatile nutrient and specific signal. Plant Physiol 136:2438–2442

Hu Y, Schmidhalter U (2001) Reduced cellular crosssectional area in the leaf elongation zone of wheat causes a decrease in dry weight

deposition under saline conditions. Aust J Plant Physiol 28:165–170

Jia Y, Yang X, Feng Y, Jilani G (2008) Differential response of root morphology to potassium deficient stress among rice genotypes varying in potassium efficiency. J Zhejiang Univ Sci B 9:427–434

Judziewicz E, Clark L, Londono X, Stern M (1999) American Bamboos. Smithsonian Institution Press, Washington DC

Junghans U, Polle A, Duchting P, Weiler E, Kuhlman B, Gruber F, Teichmann T (2006) Adaptation to high salinity in poplar involves changes in xylem anatomy and auxin physiology. Plant Cell Environ 29:1519–1531

Kilic S, Kabar K (2007) Effects of 24-epibrassinolide on salinity stress induced inhibition of seed germination, seedling growth and leaf anatomy of barley. SDU Fac Arts Sci J Sci 2:41–52

Lauchli A, Grattan SR (2007) Plant growth and development under salinity stress. In: Jenks MA, Hasegawa PM, Jain MS (eds) Advances in molecular breeding toward drought and salt tolerant crops. Springer, Berlin, pp 1–32

Li Y, Su X, Zhang B, Huang Q, Zhang X, Huang R (2009) Expression of jasmonic ethylene responsive factor gene in transgenic poplar tree leads to increased salt tolerance. Tree Physiol 29:273–279

Li X, Ding M, Zhou C, Liu C (2012) Evaluation of nutrient components in five bamboo shoots. J Zhejiang For Sci Technol 32:43–47

Liese W (1987) Research on bamboo. Wood Sci Technol 21:189–209

Lutts S, Kinet JM, Bouharmont J (1996) Effects of various salts and of mannitol onion and proline accumulation in relation to osmotic adjustment in rice (*Oryza sativa* L.) callus cultures. J Plant Physiol 149:186–195

Lutts S, Almansouri M, Kinet JM (2004) Salinity and water stress have contrasting effects on the relationship between growth and cell viability during and after stress exposure in durum wheat callus. Plant Sci 167:9–18

Maathuis FJM, Amtmann A (1999) K^+ nutrition and Na^+ toxicity: the basis of cellular K^+: Na^+ ratios. Ann Bot 84:123–133

Mahajan S, Tuteja N (2005) Cold, salinity and drought stresses: an overview. Arch Biochem Biophys 444:139–158

Marschner H (1995) Mineral nutrition of higher plants. Academic Press, San Diego

Marschner H, Cakmak I (1989) High light intensity enhances chlorosis and necrosis in leaves of zinc, potassium and magnesium deficient bean (*Phaseolus vulgaris*) plants. J Plant Physiol 134:308–315

Maxwell K, Johnson GN (2000) Chlorophyll fluorescence-a practical guide. J Exp Bot 51:659–668

Munns R (1993) Physiological processes limiting plant growth in saline soils: some dogmas and hypotheses. Plant Cell Environ 16:15–24

Raafat A, Habib SA, El-Shami IZ, El-Antably HM (1991) The effect of salinity on the anatomical features of tomato plants. Ann Agric Sci 36:307–321

Ramoliya PJ, Patel HM, Pandey AN (2004) Effect of salinization of soil on growth and macro-and micro-nutrient accumulation in seedlings of *Salvadora persica* (Salvadoraceae). For Ecol Manag 202:181–193

Rathinasabapathi B, Burnet M, Russell BL, Gage DA, Liao PC, Nye GJ, Scott P, Golbeck JH, Hanson AD (1997) Choline monooxygenase, an unusual iron–sulfur enzyme catalyzing the first step of glycine betaine synthesis in plants: prosthetic group characterization and cDNA cloning. Proc Natl Acad Sci USA 94:3454–3458

Reinhardt D, Rost TL (1995) On the correlation of primary root growth and tracheary element size and distance from the tip in cotton seedlings grown under salinity. Environ Exp Bot 35:575–588

Roychoudury A, Basu S, Sarkar SN, Sengupta DN (2008) Comparative physiological and molecular responses of a common aromatic indica rice cultivar to high salinity with non-aromatic indica rice cultivars. Plant Cell Rep 27:1395–1410

Sairam RK, Tyagi A (2004) Physiology and molecular biology of salinity stress tolerance in plants. Curr Sci 86:407–421

Santos-Diaz MS, Alejo-Ochoa N (1994) PEG-tolerant cell clones of chilipepper: growth, osmotic potentials and solute accumulation. Plant Cell Tissue Org 37:1–8

Satpal T, Katrina C, Shashi K (2012) Salinity tolerance in plants: breeding and genetic engineering. Aust J Crop Sci 6:1337–1348

Shabala S (2009) Salinity and programmed cell death: unraveling mechanisms for ion specific signalling. J Exp Bot 60:709–712

Shi HZ, Quintero FJ, Pardo JM, Zhu JK (2002) The putative plasma membrane Na^+/H^+ antiporter SOS1 controls long-distance Na^+ transport in plants. Plant Cell 14:465–477

Stepien P, Johnson GN (2009) Contrasting responses of photosynthesis to salt stress in the glycophyte *Arabidopsis* and the halophyte *Thellungiella*: role of the plastid terminal oxidase as an alternative electron sink. Plant Physiol 149:1154–1165

Summart J, Thanonkeo P, Prathepha P, Mcmanus MT (2010) Effect of salt stress on growth, inorganic ion and proline accumulation in Thai aromatic rice, Khao Dawk Mali 105, callus culture. Afr J Biotechnol 9:145–152

Suriyan C, Chalermpol K (2009) Effect of salt stress on proline accumulation, photosynthetic ability and growth characters in two maize cultivars. Pak J Bot 41:87–98

Tattini M, Montagni G, Traversi ML (2002) Gas exchange, water relations and osmotic adjustment in *Phillyrea latifolia* grown at various salinity concentrations. Tree Physiol 22:403–412

Turan S (2012) Light acclimation in plants: photoinhibition and photoprotection. Adv Biores 3:90–94

Tyree MT, Sperry JS (1989) Vulnerability of xylem to cavitation and embolism. Annu Rev Plant Physiol Plant Mol Biol 40:19–38

Wang K, Zhang LX, Gao M, Lv LX, Zhao YG, Zhang LS, Li BZ, Han MY, Alva AK (2013) Influence of salt stress on growth and antioxidant responses of two malus species at callus and plantlet stages. Pak J Bot 45:375–381

Weimberg R (1987) Solute adjustments in leaves of two species of wheat at two different stages of growth in response to salinity. Physiol Plant 70:381–388

Wu Z, Peter HR (2008) Flora of China illustrations Poaceae. Science Press, Beijing

Zhang C, Wang F, Huang Y (2006) Techniques for tissue culture and micropropagation of *Sasa fortunei*. China For Sci Technol 20:31–33

Zhang Y, Yang YX, Zhou XM, Jia YH, Nie LL, Zhang Y, Chen SY, Wang JA, Liu ZQ (2011) The continuous accumulation of Na^+ in detached leaf section is associated with over-expression of NTHK1 and salt tolerance in poplar plants. Funct Plant Biol 38:236–245

Zhang H, Han B, Wang T, Chen SX, Li HY, Zhang YH, Dai SJ (2012a) Mechanisms of plant salt response: insights from proteomics. J Proteome Res 11:49–67

Zhang XM, Zhao L, Larson-Rabin Z, Li DZ, Guo ZH (2012b) De novo sequencing and characterization of the floral transcriptome of *Dendrocalamus latiflorus* (Poaceae: Bambusoideae). PLoS One 7:e42082

Zhou G, Meng C, Jiang P, Xu Q (2011) Review of carbon fixation in bamboo forests in China. Bot Rev 77:262–270

Zhu JK (2001) Plant salt tolerance. Trends Plant Sci 6:66–71

Zhu Z, Chen Q, Zheng HL (2012) Physiological and proteomic characterization of salt tolerance in a mangrove plant, *Bruguiera gymnorrhiza* (L.) Lam. Tree Physiol 32:1378–1388

Zimmermann MH, Tyree MT (2002) Xylem structure and the ascent of Sap, 2nd edn. Springer, Berlin